Analytical Estimates of the Subgrid Model for a Burgers Shock

Assad A. Oberai, Carlos E. Colosqui & John Wanderer
Department of Aerospace and Mechanical Engineering
Boston University
Boston, MA 02215

Report No: 05-003

Abstract

We consider finite dimensional spectral approximations of Burgers equation when the solution is given by a shock. We evaluate the subgrid term for different definitions of a desired numerical solution, made precise by the choice of a filter. In this regard, we consider the sharp cutoff filter and exponential filters. The latter is specially useful in generating solutions with reduced Gibbs oscillations. For both these filters, we conclude that the subgrid term is represented by a wavenumber dependent viscosity comprising of a finite plateau for low wavenumbers and a cusp for wavenumbers near the cutoff. The plateau and the cusp are identified with the Reynolds and cross stress terms respectively. In addition we observe that the overall viscosity increases with decreasing order of exponential filters. This increase is specially pronounced for wavenumbers near the cutoff. Our results have implications in the design and analysis of numerical methods for the spectral approximation of conservation laws with shocks.

Contents

1 Introduction

In this article we derive subgrid models for Burgers equation when the solution is given by a single shock. Burgers equation has often been considered as a simple model for modeling systems which exhibit an inertial subrange (see for example [1]). In this respect it provides insight to modeling turbulent flows. We consider Burgers equation in the domain $]0, 2\pi[$ with periodic boundary conditions. The Fourier coefficients of the solution, denoted by u_k, satisfy the following set of coupled nonlinear ordinary differential equations.

$$\frac{\partial u_k}{\partial t} - \frac{\mathrm{i}k}{2} \sum_{n \in \mathbb{Z}} u_n u_{k-n} + \nu k^2 u_k = f_k, \quad k = -\infty, \cdots, \infty. \tag{1}$$

In the equation above, ν is the viscosity, f_k denotes the Fourier coefficient for the forcing term and $\mathbb{Z}$ is the set of all integers.

The Galerkin approximation of this equation, obtained by retaining modes with wavenumber $|k| \leq \bar{k}$, where $\bar{k}$, the cutoff wavenumber is a finite, non-zero positive integer, is given by

$$\frac{\partial \bar{u}_k}{\partial t} - \frac{\mathrm{i}k}{2} \sum_{n \in \mathbb{Z}_k(\bar{k})} \bar{u}_n \bar{u}_{k-n} + \nu k^2 \bar{u}_k = f_k, \quad k = -\bar{k}, \cdots, \bar{k}. \tag{2}$$

In this equation the sum is over the set $\mathbb{Z}_k(\bar{k})$, defined as,

$$\mathbb{Z}_k(\bar{k}) = \{n | n \in \mathbb{Z}; |n|, |k-n| \leq \bar{k}\}. \tag{3}$$

Hence the sum that appears in the non-linear term is explicitly given by

$$\sum_{n \in \mathbb{Z}_k(\bar{k})} (\cdot) = \begin{cases} \displaystyle\sum_{n=-\bar{k}+k}^{\bar{k}} (\cdot) & , k \geq 0 \\ \displaystyle\sum_{n=-\bar{k}}^{\bar{k}+k} (\cdot) & , k < 0 \end{cases} \tag{4}$$

In general the Galerkin solution is not equal to the infinite dimensional solution. That is $\bar{u}_k \neq u_k$. For small viscosity, the solution of Burgers equation exhibits sharp gradients in space and time, referred to as a shocks. In this case, if $2\pi/\bar{k}$ is smaller than the shock width, then the Galerkin solution is extremely inaccurate. In fact in this regime, for time integrators which do not add any damping, the Galerkin solution is known to “blow up”. In this manuscript, in order to improve the Galerkin approximation, we propose adding a wavenumber-dependent term to it. This yields a new numerical method given by

$$\frac{\partial \bar{u}_k}{\partial t} - \frac{\mathrm{i}k}{2} \sum_{n \in \mathbb{Z}_k(\bar{k})} \bar{u}_n \bar{u}_{k-n} + \nu k^2 \bar{u}_k + m_k = \bar{f}_k, \quad k = -\bar{k}, \cdots, \bar{k}. \tag{5}$$

In the equation above, m_k is the model term, which is added to render the solution to the finite dimensional problem more accurate. It can also be interpreted as a subgrid term, that is a term which represents the effect of modes not included in the finite dimensional problem on the modes which are included. We require that the solution to this problem be related to the exact solution via

$$\bar{u}_k = \sigma_\xi u_k, \quad k = -\bar{k}, \cdots, \bar{k}, \tag{6}$$

where $\xi = k/\bar{k}$ is a scaled wavenumber and σ_ξ is a user-defined, wavenumber dependent filter. Several filters can be expressed in this form including the sharp cutoff filter and the exponential filters described in Section 4. For convenience we also set

$$\bar{f}_k = \sigma_\xi f_k, \quad k = -\bar{k}, \cdots, \bar{k}. \tag{7}$$

Substituting (7) and (6) in (5) and then using (1), we arrive at the follwing definition for the model term

$$m_k = -\frac{\mathrm{i}k\sigma_\xi}{2}\Big(\sum_{n\in\mathbb{Z}} u_n u_{k-n} - \sum_{n\in\mathbb{Z}_k(\bar{k})} \frac{\sigma_\eta \sigma_{\xi-\eta}}{\sigma_\xi} u_n u_{k-n}\Big), \quad k = -\bar{k}, \cdots, \bar{k}, \tag{8}$$

where $\eta = n/\bar{k}$, is also a scaled wavenumber. In the following section, we derive an analytical expression for m_k when the solution is given by a shock.

2 Evaluation of the Subgrid Term

For $\nu \to 0$, the solution to the Burgers equation with the initial condition $u(x,0) = \sin x$, is given by $u_k = -\frac{\mathrm{i}}{1+t}\frac{1}{k}, k \neq 0$. We approximate this solution by

$$u_k = \begin{cases} 0 & , k = 0, \text{ or } |k| > k_\infty \\ -\dfrac{\mathrm{i}}{1+t}\dfrac{1}{k} & , \text{ otherwise} \end{cases} \tag{9}$$

Utilizing this expression in (8) we arrive at

$$m_k = \frac{\mathrm{i}k\sigma_\xi}{2(1+t)^2}\Big(\sum_{n\in\mathbb{Z}_k(k_\infty)} \frac{1}{n(k-n)} - \sum_{n\in\mathbb{Z}_k(\bar{k})} \frac{\sigma_\eta\sigma_{\xi-\eta}}{\sigma_\xi n(k-n)}\Big). \tag{10}$$

We approximate the summation in the equation above with an integral to arrive at,

$$m_k \approx \frac{\mathrm{i}k\sigma_\xi}{2(1+t)^2}\Big(\int_{\mathbb{R}_k(k_\infty)} \frac{1}{n(k-n)}dn - \int_{\mathbb{R}_k(\bar{k})} \frac{\sigma_\eta\sigma_{\xi-\eta}}{\sigma_\xi n(k-n)}dn\Big), \tag{11}$$

where

$$\mathbb{R}_k(\bar{k}) = \{n | n \in \mathbb{R}; |n|, |k-n| \leq \bar{k}\}. \tag{12}$$

Thus the integral in (11) is given by

$$\int_{\mathbb{R}_k(\bar{k})} \equiv \begin{cases} \displaystyle\int_{-\bar{k}+k}^{\bar{k}} & , k \geq 0, \\ \displaystyle\int_{-\bar{k}}^{\bar{k}+k} & , k < 0 \end{cases} \tag{13}$$

Utilizing scaled wavenumbers, $\eta = n/\bar{k}$ and $\xi = k/\bar{k}$ in (11), we arrive at

$$m_k \approx \frac{\mathrm{i}\xi\sigma_\xi}{2(1+t)^2}\Big(\int_{\mathbb{R}_\xi(\xi_\infty)} \frac{1}{\eta(\xi-\eta)}d\eta - \int_{\mathbb{R}_\xi(1)} \frac{\sigma_\eta\sigma_{\xi-\eta}}{\sigma_\xi\eta(\xi-\eta)}d\eta\Big), \tag{14}$$

where $\xi_\infty = k/k_\infty$.

We now evaluate terms in (14) such that m_k is analytically calculable for a sharp cutoff filter (that is $\sigma_\xi = 1$). We rewrite (14) as,

$$m_k \approx \frac{\mathrm{i}\xi\sigma_\xi}{2(1+t)^2}\Big(\int_{\mathbb{R}_\xi(\xi_\infty)} \frac{1}{\eta(\xi-\eta)}d\eta - \int_{\mathbb{R}_\xi(1)} \frac{1}{\eta(\xi-\eta)}d\eta + \int_{\mathbb{R}_\xi(1)} \frac{1-\sigma_\eta\sigma_{\xi-\eta}/\sigma_\xi}{\eta(\xi-\eta)}d\eta\Big). \tag{15}$$

For $k \geq 0$ the first two integrals in (15) evaluate to

$$\begin{aligned}
\int_{\mathbb{R}_\xi(\xi_\infty)} \frac{1}{\eta(\xi-\eta)}d\eta - \int_{\mathbb{R}_\xi(1)} \frac{1}{\eta(\xi-\eta)}d\eta &= \Big(\int_{-\xi_\infty+\xi}^{-1+\xi} \frac{1}{\eta(\xi-\eta)}d\eta + \int_1^{\xi_\infty} \frac{1}{\eta(\xi-\eta)}d\eta\Big) \\
&= \frac{1}{\xi}\Big(\int_{-\xi_\infty+\xi}^{-\bar{1}+\xi} (\frac{1}{\eta} + \frac{1}{\xi-\eta})d\eta + \int_1^{\xi_\infty} (\frac{1}{\eta} + \frac{1}{\xi-\eta})d\eta\Big) \\
&= \frac{2}{\xi}\ln\Big(\frac{1-\xi}{1-\xi/\xi_\infty}\Big).
\end{aligned} \tag{16}$$

similarly for $k < 0$ we obtain

$$\int_{\mathbb{R}_\xi(\xi_\infty)} \frac{1}{\eta(\xi-\eta)}d\eta - \int_{\mathbb{R}_\xi(1)} \frac{1}{\eta(\xi-\eta)}d\eta = -\frac{2}{\xi}\ln\Big(\frac{1+\xi}{1+\xi/\xi_\infty}\Big). \tag{17}$$

Combining these equation for the integrals in (15) we have the following expression for the model term

$$m_k \approx \frac{\mathrm{i}\sigma_\xi}{(1+t)^2}\Big(\mathrm{sgn}\xi \ln\big(\frac{1-|\xi|}{1-|\xi|/\xi_\infty}\big) + \frac{\xi}{2}\int_{\mathbb{R}_\xi(1)} \frac{1-\sigma_\eta\sigma_{\xi-\eta}/\sigma_\xi}{\eta(\xi-\eta)}d\eta\Big). \tag{18}$$

3 Interpretation as a Viscosity

Next, we evaluate a wavenumber-dependent viscosity ν_k that replicates the subgrid term m_k. That is

$$\nu_k k^2 \bar{u}_k = m_k. \tag{19}$$

Substituting (6), (9) and (18) in the above equation we arrive at the definition for ν_k:

$$\nu_k = -\frac{1}{\bar{k}(1+t)}\Big(\frac{1}{|\xi|}\ln\big(\frac{1-|\xi|}{1-|\xi|/\xi_\infty}\big) + \frac{\xi}{2}\int_{\mathbb{R}_\xi(1)} \frac{1-\sigma_\eta\sigma_{\xi-\eta}/\sigma_\xi}{\eta(\xi-\eta)}d\eta\Big). \tag{20}$$

Note that the scaled viscosity $\tilde{\nu}_k = \nu_k/(\frac{1}{\bar{k}(1+t)})$ is conveniently expressed in terms of the scaled values of the wavenumbers $\xi = k/\bar{k}$ and $\xi_\infty = k_\infty/\bar{k}$ as

$$\tilde{\nu}_k = -\Big(\frac{1}{|\xi|}\ln\big(\frac{1-|\xi|}{1-|\xi|/\xi_\infty}\big) + \frac{\xi}{2}\int_{\mathbb{R}_\xi(1)} \frac{1-\sigma_\eta\sigma_{\xi-\eta}/\sigma_\xi}{\eta(\xi-\eta)}d\eta\Big). \tag{21}$$

In the following section we analyze this expression for different choices of the filter σ_ξ.

4 Analysis of the subgrid viscosity

4.1 Sharp cutoff filter

For this filter $\sigma_\xi = 1$ and the integral in (21) is zero and hence the viscosity is calculable analytically. This expression is further simplified if we consider the limit $\nu \to 0$, for which $\xi_\infty \to \infty$. In this limit,

$$\tilde{\nu}_k = -\frac{1}{|\xi|} \ln \big(1 - |\xi|\big). \tag{22}$$

In Figure 1, we have plotted this viscosity as a function of the scaled wavenumber ξ. We observe that for low wavenumbers the viscosity attains an asymptote of unity. This may be inferred from (22) by employing L'Hopital's rule. For higher wavenumbers (that is $\xi \to 1$), it displays a logarithmic cusp with a singularity at $\xi = 1$. Remarkably this behavior is very similar to the cusp observed in three dimensional turbulence in the limit of an infinite inertial range (see for example [2, 3]).

It is interesting to examine the contribution from the various components of the subgrid term to this viscosity. In particular we wish to determine the contributions from the cross-stress and the Reynolds stress term (following large eddy simulation nomenclature). Recall that the cross-stress component of the subgrid term accounts for the interaction of modes outside the cutoff with modes within the cutoff. In (8) this corresponds to the case when only one of $|n|$ and $|k - n|$ is greater than $\bar{k}$. On the other hand for the Reynolds stress both the modes in the subgrid stress must be beyond the cutoff. That is in (8) both $|n|$ and $|k - n|$ are greater than $\bar{k}$. Note that for the sharp cutoff filter, the contribution from the third component, that is the Leonard stress, which only involves modes below the cutoff, is zero. According to this classification the integrals in (16) can be split into a cross-stress part, which is evaluated within the limits $(-1, -1 + \xi)$ and $(1, 1 + \xi)$, and a Reynolds stress part which is evaluated within the limits $(-\xi_\infty + \xi, -1)$ and $(1 + \xi, \xi_\infty)$. This yields a cross-stress model term, m_k^C, given by

$$m_k^C = \frac{\mathrm{i}\sigma_\xi \mathrm{sgn}\xi}{(1+t)^2} \ln \big(1 - \xi^2\big), \tag{23}$$

and a Reynolds stress term, m_k^R given by

$$m_k^R \approx -\frac{\mathrm{i}\sigma_\xi \mathrm{sgn}\xi}{(1+t)^2} \ln \big((1 + |\xi|)(1 - |\xi|/\xi_\infty)\big). \tag{24}$$

Note that by definition $m_k^C + m_k^R = m_k$.

As for the total model, these individual model terms may be represented by a wavenumber-dependent viscosity, where the scaled viscosity for the cross-stress term is given by

$$\tilde{\nu}_k^C = -\frac{1}{|\xi|} \ln \big(1 - \xi^2\big), \tag{25}$$

and for the Reynolds stress it is given by

$$\tilde{\nu}_k^R = \frac{1}{|\xi|} \ln \big((1 + |\xi|)(1 - |\xi|/\xi_\infty)\big). \tag{26}$$

Once again $\tilde{\nu}_k^C + \tilde{\nu}_k^R = \tilde{\nu}_k$. We now examine the relative contributions from these terms to the overall viscosity for low and high wavenumbers ($\xi \to 0$ and $\xi \to 1$, respectively). For simplicity, we consider the case of an infinite k^{-1} range, that is $\xi_\infty \to \infty$. In this limit, when $\xi \to 0$, $\tilde{\nu}_k^C \to 0$ and $\tilde{\nu}_k^R \to 1$. That is the plateau that appears in the total viscosity at low wavenumbers is due to the Reynolds stress terms and the contribution from the cross-stress term vanishes. Note that Reynolds stress term represents the long-range (in wavenumber space) interactions. Hence for low wavenumbers the long-range interaction are important. On the other hand, when $\xi \to 1$, that is for the wavenumbers near the cutoff, $\tilde{\nu}_k^C \to \infty$ and $\tilde{\nu}_k^R \to \ln 2$. Hence, the cusp near the cutoff wavenumber in the total viscosity is due to cross-stress terms which represents short-range or local interactions in wavenumber space. These observations are clearly seen Figure 1, where we have plotted $\tilde{\nu}_k^C, \tilde{\nu}_k^R$ and $\tilde{\nu}_k$. It is remarkable that similar observations regarding the splitting of subgrid contributions have also been made for three dimensional turbulence.

In Figure 2, we have plotted $\tilde{\nu}_k$ as a function of ξ for different values of ξ_∞, which represents the upper limit of the k^{-1} spectra of the exact solution. Note that $2\pi\xi_\infty^{-1}$ is an estimate of the width of the shock in the exact solution. We observe that with decreasing ξ_∞ (increasing shock width) the asymptote at $\xi = 0$ decreases. In fact from (21) we conclude that in this limit $\tilde{\nu}_k = 1 - \xi_\infty^{-1}$. This may be explained by examining the Reynolds stress contribution, which is the only non-zero contribution for $\xi = 0$. As ξ_∞ decreases, the number of modes which contribute to the Reynolds stress (long range interactions) also decreases and hence the magnitude of the model term and the subgrid viscosity decreases. From the figure we also observe that with decreasing ξ_∞ the range of the cusp decreases while its sharpness increases.

4.2 Gibbs phenomena

For solutions with shocks it is often desirable to generate numerical solutions with reduced Gibbs oscillations. In the previous section we required the Fourier coefficients of the solution of the modeled system and the exact system to be equal to each other up to the cutoff wavenumber. In other words, we required that the modeled solution to the equal to the exact solution operated upon by a sharp cutoff filter. It is well known that this filter does not alleviate Gibbs phenomena. On the other hand, exponential filters are quite effective in accomplishing this [4]. These filters are given by

$$\sigma_\xi = \begin{cases} e^{-\alpha\xi^p}, & |\xi| \leq 1 \\ 0, & |\xi| > 1 \end{cases} \tag{27}$$

where p is an even integer which determines the order of the filter and α is a number chosen so that $e^{-\alpha}$ is a small number close to machine precision. In Figure 3, we have plotted exponential filters of different orders ($p = 2, 4, 8, 20, 60$) with $\alpha = 15$. We observe that with increasing p, the exponential filter approaches the sharp cutoff filter. In this section we estimate the subgrid viscosity when the numerical solution is required to be the exact solution operated upon by an exponential filter.

When $\sigma_\xi \neq 1$, then the contribution from the integral in (21) is non-zero. For an exponential filter, this integral is hard to evaluate analytically. However, it is easily calculated numerically. In Figure 4, we have plotted the subgrid viscosity (on a log-scale) for exponential filters of various orders. We have also included the viscosity for the sharp cutoff filter. We observe that in general the use of an exponential filter increases the overall viscosity. In particular, it enhances the cusp at $\xi = 1$ significantly. The increase in the value at $\xi = 0$ is clearly seen in Figure 5, where we focus on lower wavenumbers. It is remarkable that the viscosity for the second order exponential filter is at least 10 times greater than the viscosity for the sharp cutoff filter across all wavenumbers. This indicates that in a spectral approximation the viscosity required for solution with reduced Gibbs phenomena is much larger than that required to achieve modal accuracy. In a broader context, this indicates that the form of the model term in a method is determined by the definition of the required numerical solution.

5 Conclusions

We have considered the spectral approximation of Burgers equation with periodic boundary conditions. For different choices of the optimal numerical solution, we have derived an analytical expression for the model term when the exact solution is given by a shock. We have found that this term can be expressed as a wavenumber dependent viscosity.

When the optimal numerical solution is defined as the exact solution operated on by a sharp cutoff filter, the subgrid viscosity is shown to have a plateau at low wavenumbers and a cusp (logarithmic singularity) at wavenumbers close to the cutoff. The plateau is a consequence of the long-range interactions in wavenumber space (Reynolds stress terms) and the cusp is formed by contributions from short range interactions (cross-stress terms). Remarkably, this picture is very close to what is observed in three dimensional turbulent flows.

We have also examined how the model term changes when the optimal solution is required to demonstrate reduced Gibbs oscillations. In this case, we have defined the optimal solution as the exact solution operated upon by an exponential filter. We have found that with decreasing order of the filter the overall viscosity increases significantly for all wavenumbers. In addition, the increase for higher wavenumbers (near the cutoff) is more pronounced. These results indicate the sensitivity of the model term on the definition of the optimal numerical solution.

Our results will be useful in designing spectral discretizations of Burgers equation. As of now, they appear to validate, to some extent, the vanishing spectral viscosity method [5]. In this method a wavenumber dependent viscosity is applied only to the higher modes in a simulation. However, they also indicate that a smaller viscosity should be applied to the lower wavenumbers (the finite plateau). In this respect they justify the dynamic multiscale method where two different non-zero viscosities are employed and determined dynamically using the variational Germano identity [6].

Acknowledgments

The support of DOE Award No. DE-FG02-04ER25648 is gratefully acknowledged.

References

[1] P. D. Lax. *Hyperbolic systems of Conservation Laws and the Mathematical Theory of Shock Waves.* Society for Industrial and Applied Mathematics, Philadelphia, PA, 1972.

[2] R.H. Kraichnan. Eddy Viscosity in Two and Three Dimensions. *Journal of the Atmospheric Sciences*, **33**:1521–1536, 1976.

[3] D. Leslie and G. Quarini. The Application of Turbulence Theory to the Formulation of Subgrid Modelling Procedures. *Journal of Fluid Mechanics*, **91**:65–91, 1979.

[4] D. Gottlieb and C-W Shu. On the gibbs Phenomenon and its Resolution. *SIAM Review*, **39(4)**:644–668, 1997.

[5] E. Tadmor. Convergence of Spectral Methods for Nonlinear Conservation Laws. *SIAM Journal of Numerical Analysis*, **26(1)**:30–44, 1989.

[6] A.A. Oberai and J. Wanderer. A Dynamic Diffusivity Method for the Spectral Approximation of Conservation Laws. *Computer Methods in Applied Mechanics and Engineering*, in press, 2005.

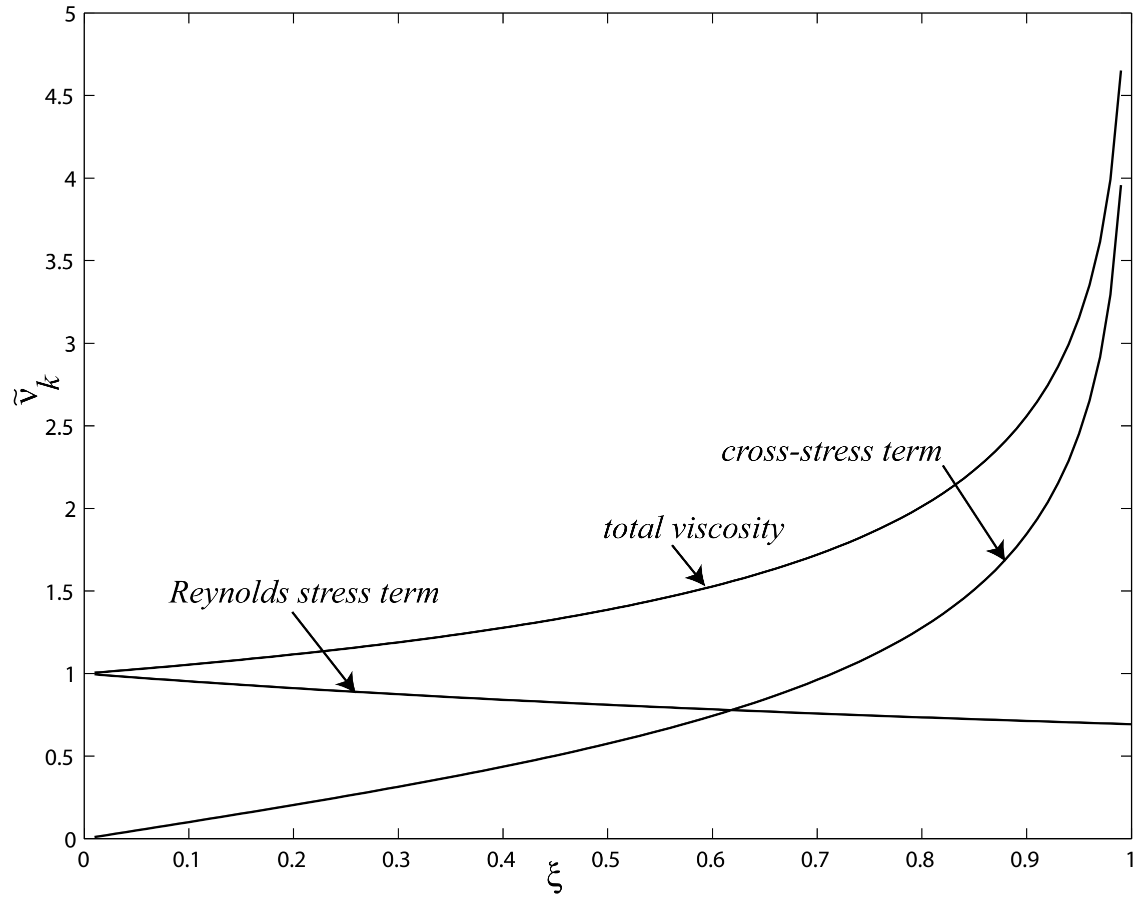

Figure 1: Different components of the scaled subgrid viscosity $\tilde{\nu}_k$ as a function of non-dimensional wavenumber ξ (for an infinite k^{-1} spectra).

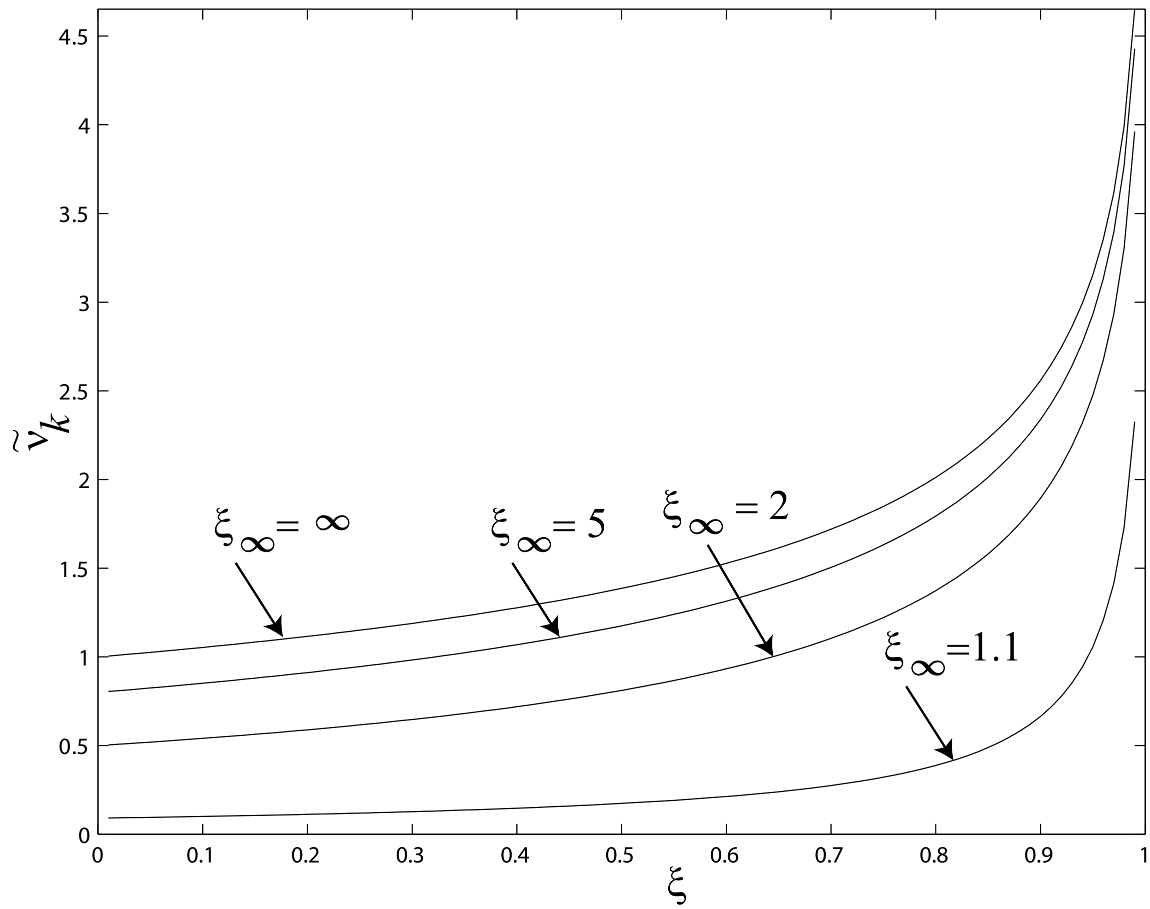

Figure 2: Scaled subgrid viscosity $\tilde{\nu}_k$ as a function of non-dimensional wavenumber ξ, for different values of ξ_∞. In this figure $\xi_\infty = 1.1, 2, 5, \infty$.

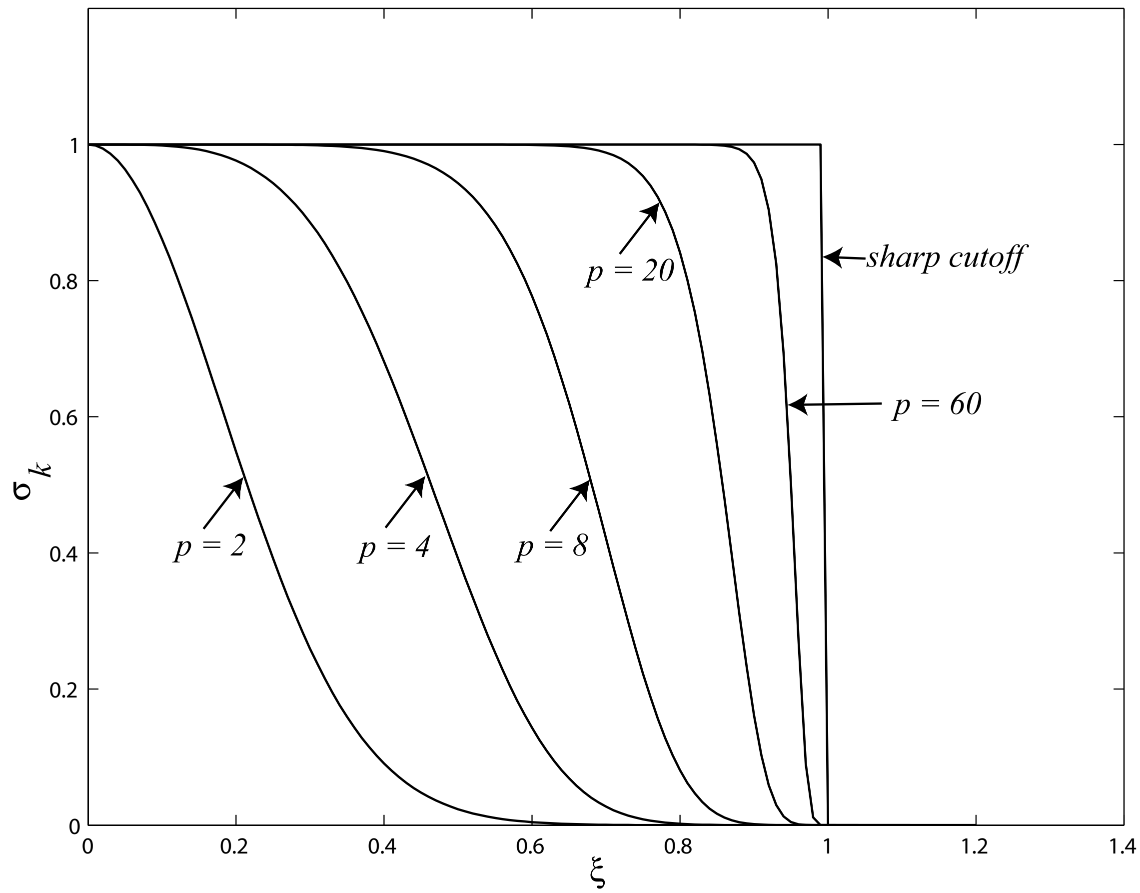

Figure 3: Exponential filters of various orders and the sharp cutoff filter.

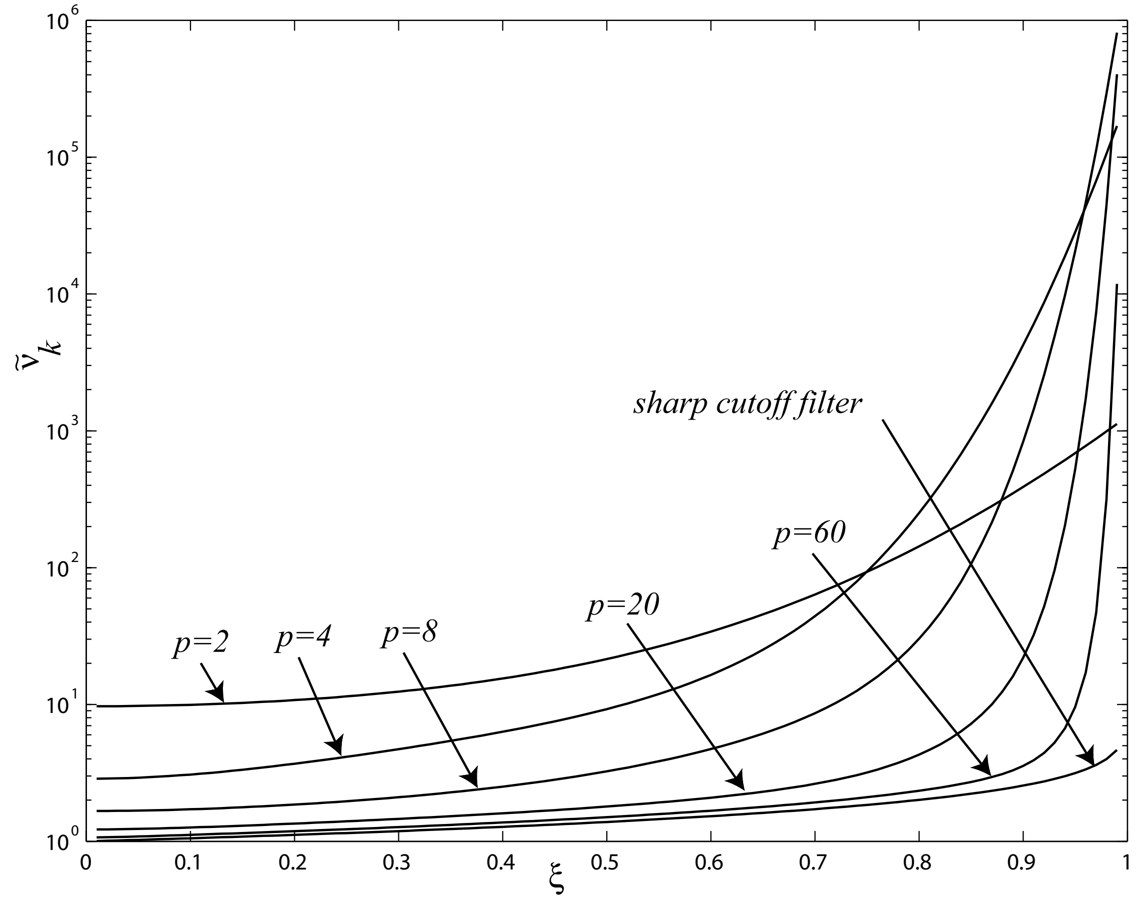

Figure 4: Scaled subgrid viscosity (logarithmic scale) for exponential filters and the sharp cutoff filter.

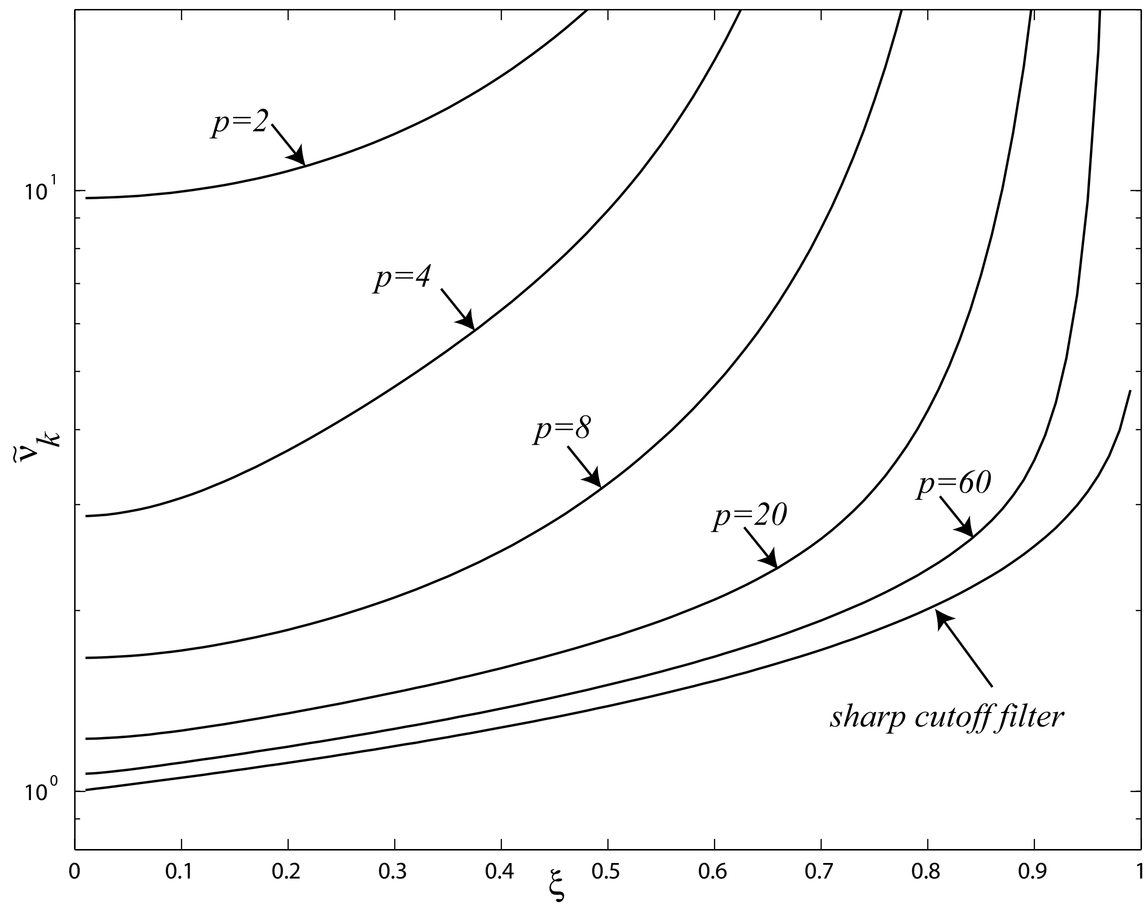

Figure 5: Scaled subgrid viscosity (logarithmic scale) for exponential filters and the sharp cutoff filter at low wavenumbers.